Canadian Science Publishing | Canadian Journal of Fisheries and Aquatic Sciences

Comparing age and growth estimates from Bayesian and integrative data approaches for the deepwater snapper Pristipomoides filamentosus in the Hawaiian Islands

Journal:	*Canadian Journal of Fisheries and Aquatic Sciences*
Manuscript ID	Draft
Manuscript Type:	Article
Date Submitted by the Author:	n/a

Complete List of Authors:	Scherrer, Stephen; University of Hawai'i at Manoa, Oceanography; Kobayashi, Don; National Marine Fisheries Service - NOAA Weng, Kevin; William & Mary Virginia Institute of Marine Science Franklin, Erik; University of Hawai'i at Manoa, Hawaii Institute of Marine Biology

Keyword:	GROWTH < General, Pristipomoides filamentous, Hawaii
Is the invited manuscript for consideration in a Special Issue? :	Not applicable (regular submission)

Introduction

Pristipomoides filamentosus (Valenciennes, 1830) is a species of long-lived deep-water snapper distributed throughout the tropical Pacific and Indian Oceans (Allen 1985; Andrews et al. 2012). Known as opakapaka in Hawaii, the species constitutes a significant fraction of the Hawaiian commercial bottomfish fishery, a complex of 6 snapper and 1 grouper species (Ralston and Polovina, 1982; Langseth et al., 2018). While the current stock assessment for this fishery used a surplus production model for the entire complex, there is interest in the potential use of species-specific, age-structured assessments that require improved life history studies of age and growth of bottomfish (Langseth et al. 2018).

Growth parameters have been estimated for *P. filamentosus* using a variety of methods in Hawaii and elsewhere (Table 2). Parameter estimates were determined using direct aging approaches from length-at-age data using otolith growth increments (Ralston and Miyamoto 1983; Uchiyama and Tagami, 1984; Radtke, 1987; DeMartini, Landgraf, and Ralston, 1994; Ralston and Williams, 1988). However, age estimates relying on the integration of daily otolith bands may be biased due to episodic growth and/or poor increment resolution in early (< 5 years) life stages (Andrews et al. 2012; Wakefield et al. 2017). Growth was also estimated using modal progression approach during a length frequency study targeting juvenile fish (< 2 years) but did not consider individual variability when extrapolating growth to larger size classes (Moffitt and Parrish 1996). Preliminary results of an ongoing tagging study have been limited by the size distribution of recaptured individuals and use model parameterizations incompatible with other methods for determining growth (O'Malley 2015). While these studies produced individual estimates of growth parameters, none of them holistically integrated across the three classes of data (direct aging, modal progression, growth increment) to explicitly evaluate the parameter values and sources of uncertainty.

Analytical and statistical advances to methods for estimating growth have been developed to account for sources of variability and permit parameter comparisons across length-at-age, length frequency, and tagging based approaches (Francis 1988; Wang et al. 1995; Eveson et al. 2004). Structural modifications to Fabens (1965) parameterization of the von Bertalanffy growth model address issues of compatibility between growth parameters estimated from tagging studies and other methods, and can reduce bias through the accommodation of modest measurement errors (Maller and Deboer, 1988; James, 1991; Palmer et al., 1991; Laslett et al., 2002; Eveson et al., 2004, 2007; Zhang et al., 2009). Maximum likelihood and Bayesian model fitting procedures accommodate individual growth variability by describing population parameters using probability distributions (Francis 1988; Kimura et al. 1993; Wang et al. 1995; Zhang et al. 2009). The flexibility of Bayesian approaches allows K and $L_\infty$to be sampled in this manner and can account for prior information when estimating parameters. Maximum likelihood approaches typically treat K as a fixed effect, but flexibility in their implementation has allowed for the development of model structures that can estimate a single set of growth parameters from direct aging, length frequency, and growth increment data simultaneously (Wang et al. 1995; Laslett et al. 2002; Eveson et al. 2004; Zhang et al. 2009).

Here, previously unreported tagging data collected in the main Hawaiian Islands (MHI) are used to estimate growth parameters for *P. filamentosus* using Bayesian and maximum likelihood procedures. A series of models integrating previous length-at-age and length frequency data collected from the MHI and Northwestern Hawaiian Islands (NWHI) with the tagging data are developed to describe growth across most of the species' life history. Models are tested to determine a preferred model structure. New growth parameters are estimated and compared to those previously reported for the Hawaiian Archipelago.

Methods

Opakapaka Tagging Program

Tagging data used for this analysis were obtained by biologists from Hawaii's Division of Aquatic Resources (DAR) within the state's Department of Land and Natural Resources (DLNR). Between 1989 and 1993, the Opakapaka Tagging Program (OTP), led by staff biologist Henry Okamoto and operating from fishing vessels contracted out of Honolulu Harbor, targeted and tagged *P. filamentosus*.

All tagging effort occurred in the main Hawaiian Islands (MHI) and was concentrated primarily around the island of Oahu and the Maui Nui complex, consisting of the islands of Maui, Molokai, Lanai, and Kahoolawe. Since 1990, these areas have accounted for approximately 67.7% of Hawaii's commercial bottomfish harvest. Coarse location data were provided in the form of the commercial statistical reporting grid areas in which individuals were tagged and recaptured (Table 1, Figure 1). Less than 1% of fish in this study were tagged off the islands of Niihau or Hawaii (Big Island). Adult bottomfish occupy depths between 100 and 400 m along undersea shelves and banks (Parke 2007). In total, the OTP tagged 4,179 juvenile and adult *P. filamentosus*.

Fish were caught with hook-and-line gear and brought to the surface at a rate of 2–5 feet per second. Prior to tagging, each fish was placed in a holding container with aerated seawater to ascertain survival likelihood. If the stomach was inverted and full of gas, it was punctured using a small sharp instrument (e.g., scalpel, hypodermic needle, fish hook). A few scales were carefully removed, and a small (~1 cm) incision was made near the fish's anal opening to assist in expelling gas from the body cavity. Fish appearing lively and upright were deemed likely to survive and thus suitable candidates for tagging. These fish were surgically implanted with unique identifiable internal anchor tags with a monofilament streamer protruding from the incision in the peritoneal cavity. The fork length of each fish measured to the nearest ¼ inch was recorded before the fish was returned headfirst to sea with enough downward momentum to assist in counteracting buoyancy caused by any residual gas.

There were 487 recaptures recorded for 439 unique individuals for a recapture rate of 10.5% of tagged fish. Recaptures of marked *P. filamentosus* were reported up to a decade after tagging with the most recent fish reported in October of 2003 (Okamoto 1993; Kobayashi et al. 2008). Individuals recaptured by OTP personnel were outfitted with an additional tag following procedures similar to their initial capture. For each individual, the location of capture (DAR statistical reporting grid), length at tagging, and date of capture were recorded. Local commercial and recreational fishers were made aware of the program through fliers distributed at the local fish markets, to fish dealers, at fishing supply outlets, and posted at small boat harbors. Fishers were incentivized to report the location, depth, fork length, and date that tagged fish were landed with a $10 reward.

Tagging Data Management

The data collected by OTP were entered into an Excel spreadsheet with subsequent analyses performed in R (R Core Team 2014), the Bayesian statistical software JAGS (Plummer 2003), and the R package R2Jags (Su and Yajima 2012). Fish were removed from the dataset if they were not the correct species of interest, if no recapture was reported, or if there was no record of the tag identification number. Fork lengths for the remaining fish recorded at tagging and recapture were linearly transformed from inches to centimeters prior to model fitting. Observed growth (Δl) and time at liberty (Δt) were calculated for each fish. If an individual was recaptured on more than one occasion, Δl and Δt were only calculated between the first marking event and the last recapture so as to not violate assumptions of independence. Fish with Δt less than 60 days were excluded from the dataset.

Parameter Estimation from Tagging Data: Bayesian Approach

Growth parameters were estimated for the *P. filamentosus* tagging data following the Bayesian methodology of Zhang et al. (2009). This approach uses a Fabens version of the von Bertalanffy growth curve but allows the parameters to vary among individuals. Hence the length upon recapture is expressed as:

$$(E1)\ \ L_{i,j} = L_{\infty,i}(1 - e^{-K_i(A_i + t_{i,j})})$$

This is parameterized such that $L_{i,j}$ is the length of individual i for the jth recapture, $t_{i,j}$ is the time-at-liberty for individual i for the jth recapture, A_i is the relative age of individual i at tagging (age minus T_0), and K_i and $L_{\infty,i}$ are the von Bertalanffy growth parameters for the ith individual. These individual parameters were drawn from Gaussian distributions defining the population mean values for K and L_∞. Uninformative priors were used for all input parameters, using Gaussian, gamma, beta, and uniform distributions following the approach of Zhang et al. (2009). The JAGS code for specifying these parameters and performing this analysis is provided in Appendix 1.

The model which allowed both the K parameter and L_∞ parameter to vary across individuals as described above is henceforth referred to as Model 1. Three additional models were run in modified versions of the JAGS code. Model 2 used a fixed K parameter while allowing the L_∞ parameter to vary across individuals. Model 3 used a fixed L_∞ parameter while allowing the K parameter to vary across individuals. Lastly, Model 4 used both a fixed K parameter and a fixed L_∞ parameter. The term "fixed" in this context does not imply a user-specified constant value, but instead refers to the value that is estimated by the Bayesian modeling approach from a single distribution used to represent the mean growth process across all individuals. Model 4 would *a priori* be most similar to the Fabens approach, with both fixed K and L_∞, but with the added feature of estimating ages at initial tagging, A_i, within the Bayesian framework. Inclusion of the A_i term represents a significant improvement over prior methods by modeling growth as a function of age, rather than observed length, allowing growth parameters to be compared between models using tagging data and length-at-age methods (Wang et al. 1995). Model 1 is the presumptive best estimate for *P. filamentosus* von Bertalanffy growth curve parameters since it would allow the most flexible incorporation of individual variability in the parameter estimation process.

For each Bayesian hierarchical model run, the first 150,000 samples from the posterior distribution were treated as burn-in and discarded from the Monte Carlo simulation. Every 50th sample from the following 1,400,000 samples (number kept = 28,000) was tabulated into the posterior distributions to reduce potential autocorrelation between sequential values or strings of values. The mean K and L_∞ values from the 28,000 kept samples were used as metrics of population mean values. Median values deviated from mean values by less than one half of 1 percent (Table 3), indicative of symmetrical distributions easily characterized by any descriptor of value tendency (i.e., mean, median, or mode). The results from the Fabens (1965) approach fit using non-linear least squares provided estimates of K and L_∞ (Table 2), which were used as initial starting points in the Bayesian hierarchical approach. Two additional chains were run, starting with initial values 50% lower and 100% higher than the initial estimates which resulted in nearly identical solutions as shown in Table 3. Convergence was also ascertained by examination of the Gelman-Rubin statistic (Gelman and Rubin 1992).

The fit of each model was assessed by calculating its Bayesian p-value from the posterior predictive distribution, and the models were compared using the DIC criterion. Bayesian p-values were derived from data simulated by model parameters and test whether simulated data are more extreme than observed data. Bayesian p-values approaching 0.5 indicate the model is a good fit to the data, while extreme Bayesian p-values near 0 or 1 indicate that a given model does not adequately represent the data (Meng 1994). Comparisons among models 1–4 were accomplished by comparing parameter estimates to model 1 where both K and L_∞ varied for individuals. If the parameter was relatively stable when allowed to be variable across individuals or fixed for the population, it might be inferred that treating this parameter on an individual basis is not warranted. However, if the parameter increased when the parameter distribution was fixed for the entire population, then it might be inferred that treating this parameter on an individual basis is necessary. Additional model comparisons were made using DIC.

Parameter Estimation from Tagging Data: Maximum Likelihood Approach

Model 5 was fit using the maximum likelihood approach of Laslett, Everson, and Polacheck (2002) using Equation 2.

$$(E2) \quad l_{ij} = \mu_\infty\left(1 - e^{-K(a_i + \Delta t_i)}\right) + \varepsilon_{ij}$$

This method derived growth parameters from the joint distribution of an individual's length at tagging and recapture to estimate growth parameters. This approach was most similar to model 2 of the Bayesian approach in that asymptotic length, L_∞, was treated as a normal random effect $N(\mu_\infty, \sigma^2_\infty)$, while K was treated as a fixed unknown parameter. The distribution of L_∞ was treated as normal, with a mean μ_∞ and standard deviation σ^2_∞, accounting for individual deviation from the population mean. Rather than using length increments to fit observed growth, a bivariate normal joint distribution of lengths recorded at marking and recapture was used to estimate each individual's age at tagging a_i. The distribution of individual a_is is A and is treated as a random effect with a lognormal distribution $L(\mu_{logA},\sigma^2_{logA})$. Measurement error was also treated as a random normal distribution $N(0, \sigma^2)$. An unconditional joint density was then derived for each individual by integrating their individual joint distribution with respect to a. A detailed description of this process is described by Laslett et al. (2002).

Growth function parameters were estimated through minimizing of the negative log-likelihood function obtained by summing the unconditional joint density $\mathrm{h}(l_1, l_2)$ of each individual (E3).

$$(E3)\ \ -\ln(\lambda_1) = -\sum_i \ln \mathrm{h}(l_{m,i}, l_{r,i})$$

This approach was used to estimate values of the parameters μ_∞, σ^2_∞, K, $\mu_{\log A}$, σ^2_{logA}, and σ^2. Two-sided 95% confidence intervals (2.5%, Median, 97.5%) were then estimated from the distribution of each parameter following 10,000 successful bootstrap iterations to obtain population parameters. For each bootstrap iteration, the model was refit on data randomly resampled from the original tagging data with replacement.

Estimation of Integrative Growth Parameters using sources of growth data

Datasets previously used to estimate regional growth for *P. filamentosus* in the MHI and NWHI and our tagging data exclusively from the MHI were used to produce a single set of parameter estimates using a modified form of the integrated method proposed by Eveson, Laslett, and Polachek (2004). Additional datasets that were included represent both direct aging and length frequency approaches.

Parameter Estimation: Length Frequency Data

Length frequency data consisted of the size distributions of juvenile *P. filamentosus* sampled over 13 months, between October 1989 and February 1991, reported by Moffitt and Parrish (1996). The reported fork length of captured fish was binned by 1 cm increments and presented in 13 histograms corresponding to each month of sampling. The number of fish of a given fork length captured during each month of sampling was determined by overlaying a series of evenly spaced horizontal lines across the Y-axis of each histogram corresponding to the addition of a single fish. Using this method to reconstruct monthly length frequency data resulted in a total count of 1,048, individuals while in the original study reported 1,047 (Moffitt and Parrish 1996).

The reconstructed length frequency data were incorporated into integrative models using the two-step method described in Laslett et al. (2004). During the first step, a Gaussian mixture model was fit using maximum likelihood and used to decompose the distribution of fork lengths from individuals sampled during discrete time periods for each cohort present in the data. This was accomplished using the normalmixEM function from the mixtools package in R (Benaglia et al. 2009) by constraining the mean of each distribution to the observed mode. A bimodal Gaussian mixture model was fit for the months of October–February, as the original study reported that two cohorts were present during this period, while a single cohort was present the remainder of the year. The estimated mean fork length, $\hat{\mu}_{ijk}$, and standard error, s_{ijk}, of each cohort during each sampling period was used to estimate growth parameters (E4).

$$(E4) \quad \hat{\mu}_{ijk} = \mu_{\infty}\left(1 - e^{-K(a_{ijk} - a_0)}\right) + e_{ijk} + \varepsilon_{ijk}$$

With this model, i, j, and k reflect the fishing year, month, and age cohort, respectively. The estimated age of each cohort during a sampling period is denoted by a_{ijk}. July is the month of peak spawning for *P. filamentosus* (Luers et al. 2017) which resulted in age estimates between 3 and 19 months. Sampling and residual model errors were described using random normal distributions $e_{ijk} \sim N(0, s_{ijk}^2)$ and $\varepsilon_{ijk} \sim N(0, \sigma_{\varepsilon}^2)$, respectively. In contrast to tagging and direct aging components, there is a dearth of information available to estimate the variance component of asymptotic length, L_{∞}, using length frequency methods, so this term was modeled as fixed effect, μ_{∞}. From this, the expected mode fork length of each cohort (E6), and associated variability during each sampling period (E7) were calculated and used to construct the negative log likelihood function (E8). The rationale for these approximations is discussed to greater depth in Eveson et al., (2004).

$$(E6) \quad E(\hat{\mu}_{ijk}) = \mu_{\infty}\left(1 - e^{-K(a_{ijk} - a_0)}\right)$$

$$(E7) \quad V(\hat{\mu}_{ijk}) = s_{ijk}^2 + \sigma_{\varepsilon}^2$$

$$(E8) \quad -\ln(\lambda_2) = \frac{1}{2}\sum_{i}\sum_{j}\sum_{k}\left[\ln\left(2\pi V(\hat{\mu}_{ijk})\right) + \frac{\left(\hat{\mu}_{ijk} - E(\hat{\mu}_{ijk})\right)^2}{V(\hat{\mu}_{ijk})}\right]$$

Parameter Estimation: Direct Aging Data

Sources of direct aging data consisted of four previously reported length-at-age datasets from three studies. Age estimates for length at age data were obtained through analytical integration of otolith bands (Ralston and Miyamoto, 1983; n = 65), counts of otolith micro increments (DeMartini et al., 1994; n = 35), comparison of bomb radiocarbon ($\Delta^{14}C$) derived from otoliths relative to a standard reference obtained from hermatypic coral cores from the Hawaiian Archipelago (Andrews et al., 2012; n = 33), and the lead-radium ratios of individuals pooled by size class (Andrews et al., 2012; n = 3).

Details of the method for estimating growth parameters from direct aging data components are described in Eveson et al. 2004. Briefly, parameters were modeled using the VBGF model described by equation E9.

$$(E9) \quad l_i = l_{\infty i}\left(1 - e^{-K(a_i - a_0)}\right) + \gamma_i$$

Expected length for each individual and the variance of the measurement error was described by equations E10 and E11.

$$(E10) \quad E(l_i) = \mu_\infty(1 - e^{-K(a_i - a_0)})$$

$$(E11) \quad V(l_i) = \sigma_\infty^2(1 - e^{-K(a_i - a_0)})^2 + \sigma_\gamma^2$$

l_i denoted the length of the i^{th} fish, at age a_i and a_0 was a fixed parameter analogous to t_0 when a fish has a hypothetical length of zero. As with the model for tagging data, $l_{\infty i}$ was the individual asymptotic length of the i^{th} fish drawn from the random normal distribution $L_\infty = N(\mu_\infty, \sigma_\infty)$. γ_i represented the distribution of individual measurement error and was similarly random, drawn from the distribution $\gamma = N(0, \sigma_\gamma)$. Equation 12 describes the log-likelihood function derived from these equations.

$$(E12) \; -ln(\lambda_2) = \frac{1}{2}\sum_i\left[\ln\left(2\pi V(l_i)\right) + \frac{(l_i - E(l_i))^2}{V(l_i)}\right]$$

An appropriate overall objective likelihood function (E13) was then defined from the sum of the negative log-likelihood functions for tag-recapture, direct aging, length frequency, and growth increment approaches, each with its own scaling constant, β.

Defining an objective function and estimating integrative growth parameters

A single set of growth parameters best describing the data was obtained by minimizing the objective likelihood function Λ (E13).

$$\text{(E13)} \quad \Lambda = \beta_1 ln(\lambda_1) + \beta_2 ln(\lambda_2) + \beta_3 ln(\lambda_3) \ldots + \beta_n ln(\lambda_n)$$

By manipulating the value of scaling constants, how similar datasets were treated, and which datasets were included, six additional model structures were developed and evaluated (Table 4). Two approaches were used to define the scaling constants (β) within each model's objective likelihood function. The first equally weighted each likelihood function so that each data source had equal influence on the resulting parameter estimates. This was achieved by selecting a β for each data source equal to the inverse of the number of observations for the data. The second weighted each data source relative to the number of observations of that particular data set ($\beta_1 = \beta_2 = \beta_3$).

The structure of model 5 fit only tagging data from the OTP study while models 6–11 incorporated the additional length-at-age and length frequency data and differed from one another in the treatment of β coefficients, whether direct aging data sources were considered independently and assigned their own log-likelihood function or if these data sources were pooled and contributed to estimation of a single log-likelihood function. Omission of direct aging data where ages were estimated by integrating daily growth increments was also considered as this method is likely to result in underestimations of age (Table 4; Wakefield et al., 2017).

The six candidate integrative model structures (Models 6–11) were evaluated against one another using the following repeated training-testing cross validation procedure (Burman 1989) to determine the combination of model weighting, data pooling, and data sources parameter estimates that consistently best predicted observed growth from tagging data. Each model structure was trained using two-thirds of the tagging data (n = 258) selected at random while the remaining one-third (n = 129) was reserved for evaluating each model's predictive ability. Model performance was evaluated using the parameters μ_∞ and k estimated from training data, applied to the length at tagging and time at liberty of each individual in the validation set to predict length at recapture using Equation 2. The variance (s^2) between the predicted ($\widehat{L_{r,i}}$) and observed ($L_{r,i}$) length of each fish recapture was used as a metric for comparing the performance of competing model structures (E14).

$$(E14) \quad s^2 = \frac{1}{n}\sum\left(L_{ri} - \widehat{L_{ri}}\right)^2$$

The preferred model structure was the one whose estimated parameters most frequently produced the smallest variance. This procedure was repeated 10,000 times. The preferred model structure was that which most frequently reported the lowest variance across all iterations. To determine if incorporating additional data sources improved predictive performance, cross validation variances for the preferred model structure were compared to those calculated using a model structure identical to Model 5, calculated including only tagging data.

The integrative model structure that best predicted observed growth most frequently was refit using the entire data set. Two-sided 95% confidence intervals were estimated for each parameter from the results of 10,000 bootstrap iterations. As with tagging data, the procedure for resampling direct aging data was straightforward and involved random sampling with replacement from the dataset to construct pseudo data sets with an equal number of observations as the original data. Bootstrapping length frequency data were slightly more complicated with each study period in the pseudo data resampled from the corresponding period of the reconstructed study data. Each study period in the pseudo dataset contained the same number of observations as in the corresponding time period of the original study data.

Results

Opakapaka Tagging Program

Of the 4,179 *P. filamentosus* tagged, 439 individuals were recaptured at least once (10.5%, Table 1). Mortality of fish upon release appeared to be generally low, facilitated by the strong tagging selectivity for healthy fish in good condition. Some immediate mortality was observed due to sharks and cetaceans or capture stress (4 individuals). Long-term mortality was thought to be relatively low based upon the high rates of tag return spanning many years. Hydra (small cnidarian polyps) biofouling of the tags was observed for some individuals with large times at liberty, with some lesions apparent around the opening where the tag exited the body cavity. This was not thought to be a serious health issue since the fish appeared to be feeding and swimming normally.

Initial fork length at capture across all individuals ranged in size from 16.5 to 53.3 cm (mean = 31.9 cm, standard deviation (s.d.) = 5.5) and ranged from 19.1 cm and 52.8 cm (mean = 32.8, s.d. = 5.1) for fish that were later recaptured. For those fish that were later recaptured, fork length at recapture ranged between 22.9 cm and 76.2 cm (mean = 41.9, s.d. = 8.7). The minimum time at liberty for any fish between tagging and recapture was a single day while the maximum time at liberty was 10.3 years (3,748 days) (Figure 2). The mean time at liberty was 1.82 years or 666 days (s.d. = 625).

One fish was excluded from further analysis as its fork length at capture was not recorded. Seven fish were removed because the recapture date was not properly recorded. Of the remaining 432 fish recaptured, 351 were recaptured a single time, 33 fish were recaptured a total of two times, one fish recaptured 3 times, and two fish were recaptured 4 times. We also excluded from analysis 45 individuals for whom time at liberty was less than 60 days yielding a data set of 387 unique individuals.

Estimating Growth Parameters from Tagging Data: Bayesian Approach

The Bayesian hierarchical approach using the JAGS software yielded mean estimates of L_∞ and K for each of the Models 1–4 examined (Table 2). Model 1, which incorporated individual variability in both L_∞ and K, yielded mean parameter estimates of L_∞ = 59.9 cm (coefficient of variation [c.v.] = 2.59) and K = 0.32 (c.v. = 8.57). L_∞ and K parameter estimates for Model 2, where K was fixed, were 60.1 cm (c.v. = 2.74) and 0.35 (c.v. = 45.7) respectively. Under Model 3, where L_∞ was fixed and K was fit freely L_∞ = 76.9 cm (c.v. = 42.2) and K = 0.17 (c.v. = 8.62) and L_∞ = 77.3 cm (c.v. = 43.1) and K = 0.24 (c.v. = 73.1) for Model 4, where both parameters were fixed. Additional parameters for each of the four models are presented in Table 3. The Gelman-Rubin convergence criteria indicated that the model solutions were credible, with asymptotic convergence clearly occurring after ~4,000 iterations, well within the burn-in phase of the Bayesian modeling runs. All 4 models appeared to fit the the data well; the mean Bayesian p-values from all retained posterior samples for all models ranged between 0.500 and 0.501. Model 1 had the largest DIC score (10582.86), followed by model 2 (10490.96), model 3 (5033.42), and model 4 (4874.83).Treating model parameters as fixed under models 2–4 resulted in excessively large coefficients of variation suggesting that individual variability in L_∞ and K is important, with perhaps variability in L_∞ being more important based upon the response of L_∞ standard deviation from the base case of Model 1 to the constrained individual variability in Model 3 and Model 4 (Figure 3).

Parameter estimation using maximum likelihood

The maximum likelihood approach used for Model 5 successfully converged to produce estimates of μ_∞, σ^2_∞, K, $\mu_{\log A}$, σ^2_{logA}, and σ^2 (Table 5). Bootstrap confidence intervals of parameters μ_∞ and K overlapped L_∞ and K parameters from Bayesian models 1 and 2 (Table 2). From these results, it was concluded that estimates produced by maximum likelihood were satisfactorily similar to estimates from the Bayesian approach. Model residuals were distributed around zero fairly consistently for all but the largest fish. For fish with recapture lengths exceeding 60 cm, growth models underestimated observed recapture lengths (Figures 3).

Comparing model performance

Across all 10,000 cross validation iterations to determine model structure, the mean predictive variance metric ranged between 7.29 and 24.96 (mean = 14.20, s.d. = 2.20) where a lower predictive variance indicates a better model fit. From all candidate likelihood models, the structure of Model 11 best predicted cross validation data in 3,486 of 10,000 iterations. The predictive variance for Model 11 ranged between 7.29 and 20.10 (mean = 13.64, s.d. = 1.91). The structure of Model 5, fit exclusively using tagging data, ranged in predictive variance between 7.17 and 26.09 (mean = 14.35, s.d. = 2.44). The structure of Model 11 performed better than the structure of Model 5 in 6,351 of 10,000 cross validation iterations. Differences in predictive variance between these two competing structures ranged between −1.60 and 10.80

(mean = 0.72, s.d. = 1.37) and indicated that the inclusion of additional growth data did improve the predictive capability of growth models compared to tagging data alone. Bootstrapped parameter estimates that were refitted(?) using the preferred model structure and Model 5's tagging only data are summarized in Table 2 and all parameters for models 5-11 are reported in full in Table 5. When fit to the entire tagging data set, the residual pattern of Model 11 also underestimated lengths at recapture length for the largest individuals.

Discussion

Our integrative model results reconcile 30+ years of efforts to determine growth for *P. filamentosus* in the Hawaiian Archipelago and provide robust support for some observed life history parameters. Growth parameters derived using integrative models that incorporated additional length frequency and length-at-age data were better able to predict observed growth in recaptured fish. These parameters were in agreement with those derived from; (1) the fit of only integrated daily growth increments from otoliths collected in the NWHI without constraining L_∞ (Ralston and Miyamoto 1983), (2) integrated daily growth increments and microincrement counts (DeMartini et al., 1994), and (3) the radioisotopic composition of otolith material and counts of otolith increments from the MHI and NWHI (Andrews et al., 2012) and support the implicit assumption that tagging individuals did not disrupt their growth trajectory. Integrative parameters differed from estimates from an ongoing mark recapture study in the MHI which reported faster growth and smaller asymptotic lengths (O'Malley 2015). These differences could arise from real changes in growth between the periods fish were collected, methodological differences, as well as that thus far, none of the fish recaptured during the ongoing study have been of the largest size classes (maximum size reported = 47.6 cm FL).

Compared to their broader distribution, *P. filamentosus* from the Hawaiian archipelago were slower growing but obtained larger asymptotic lengths than those from the Mariana Archipelago (Ralston and Williams 1988) and Papua New Guinea (Fry et al., 2006; Andrews et al., 2012), and were faster growing but ultimately smaller in their asymptotic length when compared to estimates from the Seychelles (Mees 1993; Hardman-Mountford et al. 1997; Mees and Rousseau 1997; Pilling 2000).

Comparing growth parameter estimates fit exclusively with OTP data indicates that Bayesian and maximum likelihood fitting methods performed similarly. The treatement of individual variability in parameters estimated in Model 2 were identical to those used to fit Model 5 (OTP data only). Parameters estimated by Models 1 and 2 were contained within the 95% confidence intervals of Model 5. Integrative Models 6–11 were evaluated under the same assumptions of parameter variability as models 2 and 5.

Of the Bayesian models, Model 1 was the presumed optimal because it incorporated individual variability in both L_∞ and K parameters. The additional Models 2–4 suggest that individual variability in both K and L_∞ is important, with perhaps variability in L_∞ being more important based upon the response of L_∞ standard deviation from the base case of Model 1 to the constrained individual variability in Model 3 and Model 4 (Figure 3). While Models 3 and 4 had lower DIC values based upon parameter estimates and patterns of standard deviation, it is likely that these models were not credible. Similar parameter estimates obtained from Models 1 and 2 suggested that the primary source of individual variability was due to variability in the L_∞ parameter. This is consistent with other studies where the best models accounted for individual variability in both terms but accounting for individual variation in the L_∞ term alone was sufficient to describe growth while significantly reducing computational complexity (Eveson et al., 2007; Zhang et al., 2009).

Across all models, the parameters from Model 11 best predicted length at recapture across validation iterations and therefore represents the best estimated parameter set. Information from older/larger fish was very important for grounding the upper end of integrative growth curves resulting in parameters that better predicted length at recapture. Omission of the largest individuals from Models 1–5 resulted in lower estimates of L_∞, causing growth curves to asymptote prematurely. When included, additional data sources resulted in growth parameters that were better able to predict the length of fish recaptured from the MHI in the OTP study.

Additional data sources included in integrative models represent collections spanning several decades and were collected across both the MHI and NWHI. When incorporating these additional data sources, it must be assumed that growth within the population did not differ significantly with time or region. Genetic homogeneity between NWHI and MHI stocks (Gaither et al., 2010; Gaither et al., 2011) justified incorporating data from both regions and with the exception of Ralston and Miyamoto (1983), all subsequent studies of growth for *P. filamentosus* in the Hawaiian archipelago have included data or parameter estimates from one or more previous studies in their calculations regardless of time and place of collection (DeMartini et al., 1994; Moffitt and Parrish, 1996; Andrews et al., 2012). However, these spatial and temporal assumptions may not reflect phenotypic realities, and further work is required to resolve whether differences in growth exist between the two regions.

Parameters obtained from our models and those published elsewhere underestimate the size at recapture for the largest fish in the OTP dataset (approximate fork length > 50 cm) (Figure 4). Sexual size dimorphism may explain this poor predictive ability. If one sex attains a greater asymptotic length than the other, that sex is likely to be overrepresented in the largest size classes relative to the total population. At sizes where the sex ratio of individuals is similar to the sex ratio of the total sampled population, averaging of model parameters between sexes results in excess model deviation. However, for the largest sizes where sex ratios are not representative of the population as a whole, estimated growth parameters represent an average of both sexes and will underestimate recapture lengths for largest individuals from one sex while overestimating the recapture length of the largest individuals of the other. While not pronounced, dimorphic size differences have been observed in a number of lutjanid species (Grimes 1987; Mees 1993; Newman et al. 2000; Newman and Dunk 2002; Williams et al. 2017; Taylor et al. 2018; Nichols 2019). Estimations of growth parameters for *P. filamentosus* in the Central Pacific are sex agnostic, and the method for non-invasive sexing of this species was unknown until recently (Luers et al., 2017). However, elsewhere in their distribution, larger asymptotic lengths have been reported for male *P. filamentosus* in the Seychelles, while during research fishing in the Northwestern Hawaiian Islands, the number of females outnumbered males almost 2:1 in the largest size classes, and in Guam no differences between sexes were observed (Kami 1973; Kikkawa 1984; Mees 1993).

Accurate estimates of von Bertalanffy growth parameters are very important for management. Growth parameters are often used directly or indirectly in stock assessment and fisheries management (Polovina et al. 1987; Haight et al. 1993). These efforts are sensitive to both growth parameters and the model used to estimate those parameters. For example, the rate of instantaneous natural mortality M is a value of interest often inferred using empirical relationships between M and K (Ralston 1987; Jensen 1996; Thorson et al. 2017). Underestimating K will underestimate M, characterizing a stock as less productive than it actually is, while overestimating K will overestimate M. If the management regime is linked to such a flawed estimate of stock productivity, then the stock is likely to be mismanaged and under or over harvested, respectively, relative to its true biological potential. Future work to refine growth estimates for *P. filamentosus* should consider that growth trajectories may differ between males and females.

Acknowledgements

The authors would like to thank everyone involved with OTP. We are also thankful to the authors of the other studies that collected the data presented here including Frank Parrish, Robert Moffitt, Stephen Ralston, Garret Miyamoto, Allen Andrews, Edward DeMartini, Jon Brodziak, Ryan Nichols, and Robert Humphreys. Thanks to Annette Tagawa for providing the OTP mark recapture data used in this analysis. We would also like to thank Zane Zhang and Paige Eveson for providing code used to fit Bayesian and maximum likelihood models. Finally, we would like to thank Joe O'Malley and Frank Parrish for their advice and feedback during this project and Allen Andrews for reviewing our manuscript. Funding was provided by NOAA award #NA10NMF4520163 (to ECF). This is SOEST contribution ###### and HIMB contribution ####.

References

Allen, G.R. 1985. Fao Species Catalogue Vol . 6 . Snappers of the World. Fao Fish. Synopsis **6**(125): 208. doi:10.1016/0025-326X(92)90600-B.

Andrews, A.H., DeMartini, E.E., Brodziak, J., Nichols, R.S., and Humphreys, R.L. 2012. A long-lived life history for a tropical, deepwater snapper (Pristipomoides filamentosus): bomb radiocarbon and lead-radium dating as extensions of daily increment analyses in otoliths. Can. J. Fish. Aquat. Sci. **69**: 1850–1869. doi:10.1139/f2012-109.

Andrews, A.H., Humphreys, R.L., DeMartini, E.E., Nichols, R.S., and Brodziak, J. 2011. Bomb Radiocarbon and Lead-Radium Dating of Opakapaka (Pristipomoides filamentosus). *In* NOAA Technical Memorandum NMFS-PIFSC. Honolulu, HI. Available from http://www.pifsc.noaa.gov/library/pubs/admin/PIFSC_Admin_Rep_11-07.pdf.

Benaglia, T., Chauveau, D., Hunter, D.R., and Young, D. 2009. Mixtools: An R package for

analyzing finite mixture models. J. Stat. Softw. **32**(6): 1–29. Available from http://www.jstatsoft.org/v32/i06/.
Burman, P. 1989. A comparative study of ordinary cross-validation, v-fold cross-validation and the repeated learning-testing methods. Biometrika **76**(3): 503–514. doi:10.1093/biomet/76.3.503.
DeMartini, E.E., Landgraf, K.C., and Ralston, S. 1994. A recharacterizatinon of the age-length and growth relationships of Hawaiian snapper Pristipomoides filamentosus. U.S. Department of Commerce, National Oceanic and Atmospheric Administration, National Marine Fisheries Service, Southwest Fisheries Science Center, Honolulu, HI.
Eveson, J.P., Laslett, G.M., and Polacheck, T. 2004. An integrated model for growth incorporating tag–recapture, length–frequency, and direct aging data. Can. J. Fish. Aquat. Sci. **61**(2): 292–306. doi:10.1139/f03-163.
Eveson, J.P., Polacheck, T., and Laslett, G.M. 2007. Consequences of assuming an incorrect error structure in von Bertalanffy growth models: a simulation study. Can. J. Fish. Aquat. Sci. **64**(4): 602–617. doi:10.1139/f07-036.
Francis, R.I.C.C. 1988. Maximum likelihood estimation of growth and growth variability from tagging data. New Zeal. J. Mar. Freshw. Res. **22**(1): 43–51. doi:10.1080/00288330.1988.9516276.
Fry, G.C., Brewer, D.T., and Venables, W.N. 2006. Vulnerability of deepwater demersal fishes to commercial fishing: Evidence from a study around a tropical volcanic seamount in Papua New Guinea. Fish. Res. **81**(2–3): 126–141. doi:10.1016/j.fishres.2006.08.002.
Gelman, A., and Rubin, D.B. 1992. lnference from iterative simulation using multiple sequences. Stat. Sci. **7**(4): 457–472. doi:10.2307/2246093.
Grimes, C.B. 1987. Reproductive biology of the Lutjanidae: A review. *In* Tropical snappers and groupers: Biology and fisheries management. *Edited by* J.J. Polovina and S. Ralston. Westview Press, Boulder, Colorado. pp. 239–294.
Haight, W.R., Kobayashi, D.R., and Kawamoto, K.E. 1993. Biology and management of deepwater snappers of the Hawaiian a rchipelago. Mar. Fish. Rev. **55**(2): 20–27.
Hardman-Mountford, N.J., Polunin, N.V.C., and Boulle, D. 1997. Can the age of the tropical species be determined by otolith measurement?: a study using Pristipomoides filamentosus (Pisces: Lutjanidae) from the Mahe Plateau, Seychelles. Naga, ICLARM Q. **20**(2): 27–31.
Hawaii Reported Landing Tables. 2016. Available from https://www.pifsc.noaa.gov/wpacfin/hi/dar/Pages/hi_data_3.php [accessed 23 March 2018].
James, I.R. 1991. Estimation of von Bertalanffy growth curve parameters from recapture data. Biometrics **47**: 1519–1530. doi:10.2307/2532403.
Jensen, A.L. 1996. Beverton and Holt life history invariants result from optimal trade-off of reproduction and survival. Can. J. Fish. Aquat. Sci. **53**(4): 820–822. doi:10.1139/f95-233.
Kami, H.T. 1973. The Pristipomoides (Pices: lutjanidae) of Guam with notes on their biology. Micronesica **9**(1): 97–117. doi:10.1080/15235882.2014.934485.
Kikkawa, B.S. 1984. Maturation, spawning, and fecundity of Opakapaka, Pristipomoides filamentosus, in the Northwest Hawaiian Islands. University of Hawaii Sea Grant, Honolulu, HI.
Kimura, D.K., Shimada, A.M., and Lowe, S.A. 1993. Estimating von Bertalanffy growth parameters of sablefish Anoplopoma fimbria and Pacific cod Gadus macrocephalus using tag-recapture data. Fish. Bull. **91**(2): 271–280.
Kobayashi, D.R., Okamoto, H.Y., and Oishi, F.G. 2008. Movement of the deepwater snapper

opakapaka, Pristipomoides filamentosus, in Hawaii: Insights from a large-scale tagging program and computer simulation.

Langseth, B., Syslo, J., Yau, A., Kapur, M., and Brodziak, J. 2018. Stock assessment for the main Hawaiian Islands Deep 7 bottomfish complex in 2018, with catch projections through 2022. NOAA Tech. Memo. NMFS-PIFSC **69**(February): 217.

Laslett, G.M., Eveson, J.P., and Polacheck, T. 2002. A flexible maximum likelihood approach for fitting growth curves to tag-recapture data. Can. J. Fish. Aquat. Sci. **59**(6): 976–986. doi:10.1139/f02-069.

Luers, M.A., DeMartini, E.E., and Humphreys, R.L.J. 2017. Seasonality, sex ratio, spawning frequency and sexual maturity of the opakapaka Pristipomoides filamentosus (Perciformes: Lutjanidae) from the Main Hawaiian Islands: fundamental input to size-at-retention regulations. Mar. Freshw. Res. **69**(2): 325–335. doi:10.1071/MF17195.

Maller, R.A., and Deboer, E.S. 1988. An analysis of two methods of fitting the von Bertalanffy curve to capture-recapture data. Mar. Freshw. Res. **39**(4): 459–466. doi:10.1071/MF9880459.

Mees, C.C. 1993. Population biology and stock assessment of Pristipomoides filamentosus on the Mahe Plateau, Seychelles. J. Fish Biol. **43**(5): 695–708. doi:10.1111/j.1095-8649.1993.tb01147.x.

Mees, C.C., and Rousseau, J.A. 1997. The potential yield of the lutjanid fish Pristipomoides filamentosus from the Mahe Plateau, Seychelles: Managing with uncertainty. Fish. Res. **33**(1–3): 73–87. doi:10.1016/S0165-7836(97)00069-6.

Meng, X.-L. 1994. Posterior predictive p-values. Ann. Stat. **22**(3): 1142–1160.

Moffitt, R.B., and Parrish, F.A. 1996. Habitat and life history of juvenile Hawaiian pink snapper, Pristipomoides filamentosus. Pacific Sci. **50**(4): 371–381.

Newman, S.J., Cappo, M., and Williams, D.M.B. 2000. Age, growth and mortality of the stripey, Lutjanus carponotatus (Richardson) and the brown-stripe snapper, L. vitta (Quoy and Gaimard) from the central Great Barrier Reef, Australia. Fish. Res. **48**(3): 263–275. doi:10.1016/S0165-7836(00)00184-3.

Newman, S.J., and Dunk, I.J. 2002. Growth, age validation, mortality, and other population characteristics of the red emperor snapper, Lutjanus sebae (Cuvier, 1828), off the Kimberley coast of north-western Australia. Estuar. Coast. Shelf Sci. **55**(1): 67–80. doi:10.1006/ecss.2001.0887.

Nichols, R.S. 2019. Sex-specific growth and longevity of "Ehu", Etelis carbunculus (Family lutjanidae) within the Hawaiian archipelago. University of Hawaii.

O'Malley, J. 2015. A Review of the Cooperative Hawaiian Bottomfish Tagging Program of the Pacific Islands Fisheries Science Center and the Pacific Islands Fisheries Group. Honolulu, HI. doi:10.7289/V59W0CF7.

Okamoto, H.Y. 1993. Develop opakapaka (pink snapper) tagging techniques to assess movement behavior. Honolulu, HI.

Palmer, M.J., Phillips, B.F., and Smith, G.T. 1991. Application of nonlinear models with random coefficients to growth data. Biometrics **47**: 623–635. doi:10.2307/2532151.

Parke, M. 2007. Linking Hawaii Fisherman Reported Commercial Bottomfish Catch Data to Potential Bottomfish Habitat and Proposed Restricted Fishing Areas using GIS and Spatial Analysis. *In* NOAA Technical Memorandum NMFS-PIFSC-11. Honolulu, HI.

Pilling, G.M. 2000. Validation of annual growth increments in the otoliths of the lethrinid Lethrinus mahsena and the lutjanid Aprion virescens from sites in the tropical Indian Ocean, with notes on the nature of growth increments in Pristipomoides filamentosus. Fish. Bull. **98**(3): 600–611.

Plummer, M. 2003. JAGS: A program for analysis of Bayesian graphical models using Gibbs sampling. In Proceedings of the 3rd international workshop on distributed statistical computing. *In* Proceedings of the 3rd international workshop on distributed statistical computing. Vol. 124.

Polovina, J.J., Ralston, S., and Ralston, S. 1987. Assessment and management of deepwater bottom fishes in Hawaii and the Marianas. Trop. snappers groupers Biol. Fish. Manag.: 505–532.

R Core Team. 2014. R: A Language and Environment for Statistical Computing. Vienna, Austria. Available from http://www.r-project.org/.

Radtke, R.L. 1987. Age and growth information available from the otoliths of the Hawaiian snapper, Pristipomoides filamentosus. Coral Reefs **6**(1): 19–25. doi:10.1007/BF00302208.

Ralston, S., and Miyamoto, G.T. 1983. Analyzing the width of daily otolith increments to age the Hawaiian snapper, Pristipomoides filamentosus. Fish. Bull. **81**: 523–535.

Ralston, S. V., and Williams, H.A. 1988. Depth distributions, growth, and mortality of deep slope fishes from the Mariana archipelago.

Ralston, S.V.D. 1987. Mortality rates of snappers and groupers. Trop. snappers groupers Biol. Fish. Manag.: 375–404.

Ralston, S.V.D., and Polovina, J. 1982. A multispecies analyis of the commercial deep-sea handline fishery in Hawaii. Fish. Bull. **80**(3): 435–448.

Su, Y., and Yajima, M. 2012. R2jags: A Package for Running JAGS from R. Available from http://cran.r-project.org/package=R2jags.

Taylor, B.M., Oyafuso, Z.S., Pardee, C.B., Ochavillo, D., and Newman, S.J. 2018. Comparative demography of commercially-harvested snappers and an emperor from American Samoa. PeerJ **6**: e5069. doi:10.7717/peerj.5069.

Thorson, J.T., Munch, S.B., Cope, J.M., and Gao, J. 2017. Predicting life history parameters for all fishes worldwide. Ecol. Appl. **27**(8): 2262–2276. doi:10.1002/eap.1606.

Uchiyama, J.H., and Tagami, D.T. 1984. Life history, distribution, and abundance of bottomfishes in the Northwestern Hawaiian Islands. *In* Proceedings of the Second Symposium on Resource Investigations in the Northwestern Hawaiian Islands. *Edited by* R.W. Grigg and K.Y. Tanoue. pp. 229–247.

Wakefield, C.B., O'Malley, J.M., Williams, A.J., Taylor, B.M., Nichols, R.S., Halafihi, T., Humphreys, R.L., Kaltavara, J., Nicol, S.J., and Newman, S.J. 2017. Ageing bias and precision for deep-water snappers: Evaluating nascent otolith preparation methods using novel multivariate comparisons among readers and growth parameter estimates. ICES J. Mar. Sci. **74**(1): 193–203. doi:10.1093/icesjms/fsw162.

Wang, Y.-G., Thomas, M.R., and Somers, I.F. 1995. A maximum likelihood approach for estimating growth from tag–recapture data. Can. J. Fish. Aquat. Sci. **52**(2): 252–259. doi:10.1139/f95-025.

Williams, A.J., Wakefield, C.B., Newman, S.J., Vourey, E., Abascal, F.J., Halafihi, T., Kaltavara, J., and Nicol, S.J. 2017. Oceanic, Latitudinal, and Sex-Specific Variation in Demography of a Tropical Deepwater Snapper across the Indo-Pacific Region. Front. Mar. Sci. **4**(December). doi:10.3389/fmars.2017.00382.

Zhang, Z., Lessard, J., and Campbell, A. 2009. Use of Bayesian hierarchical models to estimate northern abalone, Haliotis kamtschatkana, growth parameters from tag-recapture data. Fish.

Res. **95**(2–3): 289–295. doi:10.1016/j.fishres.2008.09.035.

Table Captions

Table 1. Estimates of von Bertalanffy Parameters.

Estimated parameters include average asymptotic length (L_∞) the Brody growth coefficient (k), and theoretical age at length zero t0 for P. filamentosus estimated in the Main Hawaiian Islands (MHI), Northwestern Hawaiian Islands (NWHI) and pooled across the Hawaii Archipelago. When available in the literature, 95% confidence intervals for parameter estimates are presented in brackets under to parameter point estimates.

Table 2. Summary of OTP Tagging and Recapture Data for Fish with Valid Locations.

Release and recapture location numbers correspond to the State of Hawaii's statistical reporting grids (Figure 5.1). Adapted from Kobayashi, Okamoto & Oishi (2008).

Table 3. Bayesian Hierarchical Growth Model Specifications.

Monte Carlo simulation was burned in for n=10,000 runs with every 50th of the following 500,000 runs retained for tabulation into the posterior distributions. Variable names are kept consistent with the Appendix 5.1 JAGS code and are not consistent with text references to von Bertalanffy growth parameters but remain intuitively similar (e.g., Brody Growth Coefficient = K = k_mu, Asymptotic Length = L∞ = Linf_mu).

Table 4. Integrative Model Structures.

A reference for the candidate model structures used to determine the preferred integrative model structure.

Table 5. Sample and Population Parameter Estimates from Maximum Likelihood Growth Models.

Model 5 was fit to only the tagging data and Model 11 is the preferred model. For both models, parameter estimates fit to the full data set are reported in the Sample Estimate columns while bootstrapped parameter estimates (Median, 2.5%, 97.5%) are reported under the Population CI column.

Figure Captions

Figure 1. Reporting Grid Map.

Map showing the location and number of the State of Hawaii's statistical reporting grids corresponding to the reported location of tagging and recaptured for fish summarized in Table 5.2.

Figure 2. Length and Time at Liberty for OTP Data.

The length of P. filamentosus recaptured and included in analysis of OTP tagging data and the distribution of times at liberty. The fork length of fish during tagging is highlighted in red while length at recapture is shown in blue.

Figure 3. Coefficient of Variation for von Bertalanffy Growth Function Parameters.

Coefficient of variation for 2 von Bertalanffy growth function parameters (Brody growth coefficient, K) and (Mean asymptotic length $L\infty$) for P. filamentosus. Individual variability was examined incorporating individual variability in both parameters, in either one of the parameters in series, or in neither parameter.

Figure 4. Plots Comparing Predicted and Observed Length at Recapture.

Predicted lengths at recapture fit using parameter point estimates from Bayesian Models 1 and 2 and population parameter estimates from Maximum likelihood Models 5 and 11 compared to observed length at recapture. Length at recapture was predicted as a function of length at marking and time at liberty. The 1:1 line indicates where points would fall if model parameters perfectly predicted length at recapture.

TAGGING LOCATION	127	304	306	307	308	309	311	312	313	320	321	327	331	332	351
127							1								
304				1						2					
306			1							1					
307				5								1			
308			1		2						5				
309											2				
311							25	1					4		
312							1	1							
313				1				1					3		
320			1	3						24		1			
321											31				
327				3						2		2			
331							46	2					128		
332													1		
351													1		
401															
402															
403															
404															
405							1								
407													1		
408													1		
409															
421															
423											1				
424					1								4		
428							2	1					2		
429							2				1		1		
452											1		1		
505										1					
528							2								
No Recovery	1	3	44	278	35	2	582	168	5	333	429	84	875	1	1
Total	**1**	**3**	**47**	**291**	**38**	**2**	**662**	**174**	**5**	**363**	**470**	**88**	**1022**	**1**	**1**

SE LOCATION

401	402	403	404	405	407	408	409	421	423	424	428	429	452	505	528	Total
																1
																3
																2
																6
																8
																2
																30
																2
																5
																29
																31
																7
4																**180**
																1
																1
131																**131**
1																**1**
1																**1**
						1										**1**
						1										**2**
						12										**13**
																1
4								1								**5**
14						1										**15**
14						1										**16**
3						3										**11**
																5
1																**5**
																2
																1
																2
937	7	1	1	2	2	293	4	20	16	9	8	5	2	1	2	**4151**
1110	**7**	**1**	**1**	**2**	**2**	**312**	**4**	**21**	**16**	**9**	**8**	**5**	**2**	**1**	**2**	**4671**

	Method	Region	Otolith Growth Ba	Otoliths (P	Po
Direct Aging	Daily Increments	NWHI	17	-	-
	Daily Increments	NWHI	N.R.	-	-
	Daily Growth Integration	NWHI	64	-	-
	Daily Growth Integration	NWHI	64	-	-
	Daily Increments & Integration	NWHI	N.R.	-	-
	Daily Increments & Integration	MHI & NWHI	92	-	-
	Annual Increments	NWHI	N.R.	-	-
	Daily Increments, Integration, & Radioisotopes	MHI & NWHI	100	33	3
	Modal Progression	MHI	-		-
	Mark Recapture	MHI	-		-

Growth Increment	Mark Recapture	MHI	-		-
	Mark Recapture	MHI	-		-
	Mark Recapture	MHI	-		-
	Mark Recapture	MHI	-		-
	Mark Recapture	MHI	-		-
	Mark Recapture	MHI	-		-
	Mark Recapture	MHI	-		-
	Integrative	MHI & NWHI	113	33	3

Monthly Length Frequency	Recaptured Fish	Linf (95% CI)	K (95% CI)	t_o (95% CI)
-	-	-	-	-
-	-	80.5	0.16	-
-	-	78	0.146	-1.67
-	-	66.4	0.235	-0.81
-	-	69.8	0.534	0.18
-	-	70.4 (63.9 - 76.9)	0.25 (0.20, 0.31)	-0.22 (-0.39, -0.06)
-	-	97.1	0.31	0.02
-	-	67.5 (65.7, 69.3)	0.242 (0.185, 0.299)	-0.29 (-0.38, -0.20)
13		78	0.21	0
-	96	71.55	0.15	-

-	96	57.80 (55.97, 58.67)	0.28 (0.25, 0.31)	-
-	387	65.92 (60.9 - 71.6)	0.24 (0.19 - 0.30)	-
-	387	59.7 (56.9 - 63.0)	0.32 (0.27 - 0.38)	-
-	387	60.2 (57.3 - 61.2)	0.35 (0.07 - 0.39)	-
-	387	76.8 (13.7 - 162.7)	0.17 (0.14 - 0.20)	-
-	387	77.3 (12.36 - 162.7)	0.24 (0.04 - 0.76)	-
-	387	61.0 (56.1, 66.7)	0.30 (0.23, 0.39)	-
13	378	67.6 (65.4, 69.6)	0.22 (0.12, 0.25)	-0.37 (-0.47, -0.28)

Source
Moffitt (1980)
Ralston (1980)
Ralston & Miyamoto (1983) - Constrained Linf
Ralston & Miyamoto (1983) - Unconstrained Linf
Radtke (1987)
DeMartini et al. (1994)
Uchiyama & Tagami (1984)
Andrews et. al (2012)
Moffit & Parrish (1996) - Constrained Linf
O‘Malley (2015) - Gulland and Holt

O'Malley (2015) - Francis

Present Study
Francis
Present Study
Bayesian Model 1
Present Study
Bayesian Model 2
Present Study
Bayesian Model 3
Present Study
Bayesian Model 4
Present Study
Maximum Likelihood Model 5

Present Study - Integrative Model 11

	Parameter
Model 1	Linf_mu
	Linf_std
	Linf_tau
	Shape
	deviance
	k_mu
	k_std
	k_tau
	rate
	tau
	variance
Model 2	Linf_mu
	Linf_std
	Linf_tau
	Shape
	deviance
	k_mu
	k_std
	k_tau
	rate
	tau
	variance
Model 3	Linf_mu
	Linf_std
	Linf_tau
	Shape
	deviance
	k_mu
	k_std
	k_tau
	rate
	tau
	variance
	Linf_mu
	Linf_std

Model 4	Linf_tau
	Shape
	deviance
	k_mu
	k_std
	k_tau
	rate
	tau
	variance

Mean	SD	2.50%	Median	97.50%
59.89	1.58	57.10	59.80	63.24
5.47	0.34	4.80	5.46	6.15
0.03	0.00	0.03	0.03	0.04
26.85	4.40	19.63	26.36	36.86
3351.95	120.29	3106.84	3355.69	3575.02
0.32	0.03	0.27	0.32	0.37
0.01	0.00	0.01	0.01	0.02
10741.60	7970.11	2241.98	8492.59	32025.77
10.52	1.59	7.88	10.35	14.10
0.27	0.04	0.20	0.26	0.36
3.85	0.60	2.77	3.82	5.11
60.12	1.62	57.21	60.04	63.52
5.50	0.34	4.85	5.50	6.17
0.03	0.00	0.03	0.03	0.04
26.64	4.21	19.63	26.24	36.04
3356.96	119.45	3110.59	3361.29	3578.22
0.35	0.16	0.07	0.32	0.79
1.14	85.41	0.01	0.10	3.24
1294.41	3430.44	0.10	105.30	10874.77
10.36	1.49	7.85	10.22	13.67
0.26	0.04	0.19	0.26	0.36
3.88	0.60	2.77	3.85	5.14
76.89	31.95	17.19	74.42	160.86
88.68	4772.30	0.01	1.32	364.22
570.00	2323.38	0.00	0.57	6238.55
62.32	13.32	41.03	60.49	92.62
3937.75	46.81	3847.12	3937.23	4030.55
0.17	0.01	0.14	0.17	0.20
0.02	0.00	0.01	0.02	0.03
2543.07	807.09	1398.95	2400.92	4491.85
17.93	3.84	11.85	17.41	26.63
0.13	0.01	0.11	0.13	0.15
7.92	0.61	6.80	7.89	9.20
77.32	33.39	13.20	74.63	166.14
132.25	9204.30	0.01	1.65	429.54

529.45	2244.18	0.00	0.37	5947.71
32.76	3.60	26.33	32.55	40.48
4090.50	39.61	4016.26	4089.51	4171.26
0.24	0.18	0.04	0.18	0.77
5.93	1357.98	0.01	0.09	3.67
1293.51	3336.91	0.07	115.99	10767.12
9.24	0.95	7.53	9.18	11.25
0.11	0.01	0.09	0.10	0.12
9.57	0.67	8.34	9.54	10.98

Rhat	n eff
1.00	2000.00
1.00	36000.00
1.00	36000.00
1.00	2500.00
1.00	3700.00
1.00	1800.00
1.00	38000.00
1.00	38000.00
1.00	2800.00
1.00	5700.00
1.00	5700.00
1.00	30000.00
1.00	84000.00
1.00	84000.00
1.00	7900.00
1.00	28000.00
1.00	63000.00
1.00	84000.00
1.00	84000.00
1.00	5200.00
1.00	21000.00
1.00	21000.00
1.00	84000.00
1.00	84000.00
1.00	84000.00
1.00	1400.00
1.00	41000.00
1.00	3200.00
1.00	8000.00
1.00	8000.00
1.00	1600.00
1.00	84000.00
1.00	84000.00
1.00	25000.00
1.00	84000.00

1.00	84000.00
1.00	13000.00
1.00	34000.00
1.00	84000.00
1.00	84000.00
1.00	84000.00
1.00	21000.00
1.00	45000.00
1.00	45000.00

Data Source	Model 5	Model 6
Growth Increment **OTP** **Mark Recapture**	X	X
Direct Aging **Ralston & Miyamoto (1983)** **Integrated Daily Otolith Counts**	-	X
Direct Aging **Demartini et al. (1994)** **Otolith Microincrements**	-	X
Direct Aging **Andrews et al. (2012)** **Bomb Carbon**	-	X
Direct Aging **Andrews et al. (2012)** **Lead:Radium**	-	X
Length Frequency **Moffitt & Parrish (1996)** **Modal Progression**	-	X
Weighting	NA	Equal
Pooled Within Data Types?	NA	Yes

Model 7	Model 8	Model 9	Model 10	Model 11
X	X	X	X	X
X	X	X	-	-
X	X	X	X	X
X	X	X	X	X
X	X	X	X	X
X	X	X	X	X
By n	Equal	By n	Equal	By n
Yes	No	No	No	No

Parameter Estiamtes for Int

Parameter	Model 5 Sample	Model 5 Population	Model 6 Sample	Model 6 Population
Linf_mu	60.92	60.98 (56.17,66.67)	77.96	66.79 (70.27, 78.69)
Linf_std	5.32	5.3 (4.53,6.07)	6.02	5.256 (4.00, 6.83)
K	0.300	0.299 (0.229,0.393)	0.122	0.189 (0.121, 0.235)
A_mu	0.95	0.95 (0.8,1.09)	1.5	1.21 (1.06, 1.50)
A_sig	0.19	0.19 (0.15,0.24)	0.13	0.16 (0.12, 0.19)
Sig	2.1	2.08 (1.50,2.55)	2.97	2.51 (2.05, 3.11)
t0	-	-	-0.86	-0.50 (-0.90, -0.34)
oto_sig	-	-	6.79	3.93 (1.31, 7.09)
lf_sig	-	-	1.33	3.06 (1.31, 4.06)

Parameter	Model 9 Sample	Model 9 Population	Model 10 Sample	Model 10 Population
Linf_mu	64.74	64.80 (62.22, 67.03)	69.34	68.72 (65.23, 71.68)
Linf_std	5.62	5.58 (4.74, 6.37)	4.26	4.08 (3.00, 5.11)
K	0.261	0.26 (0.23, 0.30)	0.146	0.17 (0.13, 0.21)
A_mu	1	1.00 (0.925, 1.08)	1.5	1.37 (1.19, 1.60)
A_sig	0.18	0.18 (0.15, 0.22)	0.14	0.155 (0.119, 0.184)
Sig	2.2	2.20 (1.75, 2.61)	3.29	2.99 (2.45, 3.62)
t0	-0.31	-0.32 (-0.43, -0.21)	-0.8	-0.65 (-0.96, -0.43)
oto_sig	1.82	1.74 (0.66, 2.94)	1.61	1.42 (0.97, 1.84)
lf_sig	4.07	4.38 (3.88, 4.94)	1.43	2.41 (1.43, 3.29)

:egrated Growth Models

Model 7		Model 8	
Sample	**Population**	**Sample**	**Population**
64.74	64.80 (61.91, 67.17)	66.87	66.89 (63.90, 70.10)
5.62	5.57 (4.72, 6.36)	5.53	5.31 (2.61, 6.25)
0.262	0.260 (0.231, 0.302)	0.253	0.25 (0.21, 0.29)
1	1.00 (0.92, 1.08)	0.99	0.98 (0.89, 1.10)
0.18	0.18 (0.14, 0.22)	0.18	0.18 (0.15, 0.21)
2.2	2.20 (1.74, 2.62)	2.32	2.36 (1.94, 2.93)
-0.31	-0.32 (-0.44, -0.20)	-0.27	-0.27 (-0.43, -0.17)
1.82	1.76 (0.68, 3.03)	1.33	1.30 (0.47, 3.14)
4.07	4.39 (3.86, 4.98)	3.93	4.32 (3.53, 5.03)

Model 11	
Sample	**Population**
68.52	67.55 (65.42,69.55)
4.22	5.00 (4.26,5.68)
0.173	0.219 (0.198,0.245)
1.34	1.11 (1.03,1.19)
0.16	0.17 (0.14,0.2)
2.9	2.39 (2,2.77)
-0.63	-0.37 (-0.47,-0.28)
1.4	0.96 (0.49,1.31)
3.09	4.63 (4.15,5.15)

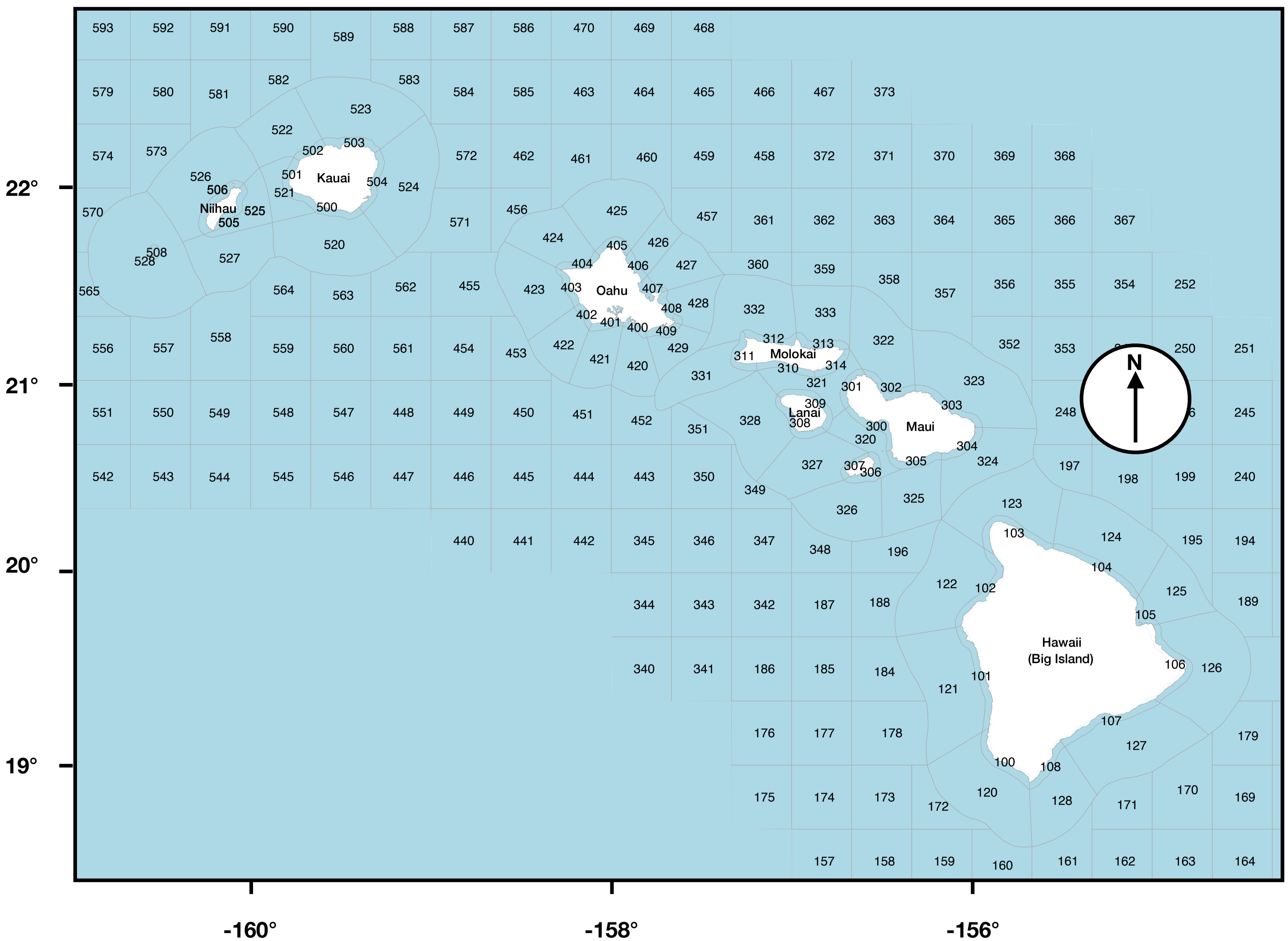
N
Kauai
Niihau
Oahu
Molokai
Lanai
Maui
Hawaii
(Big Island)
22°
21°
20°
19°
-160°
-158°
-156°

Canadian Journal of Fisheries and Aquatic Sciences

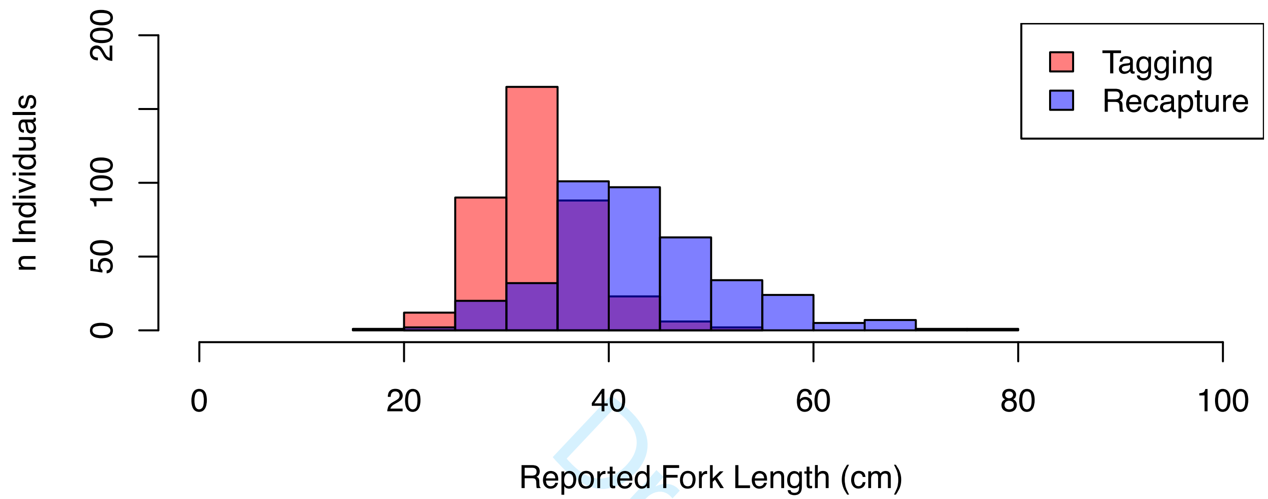

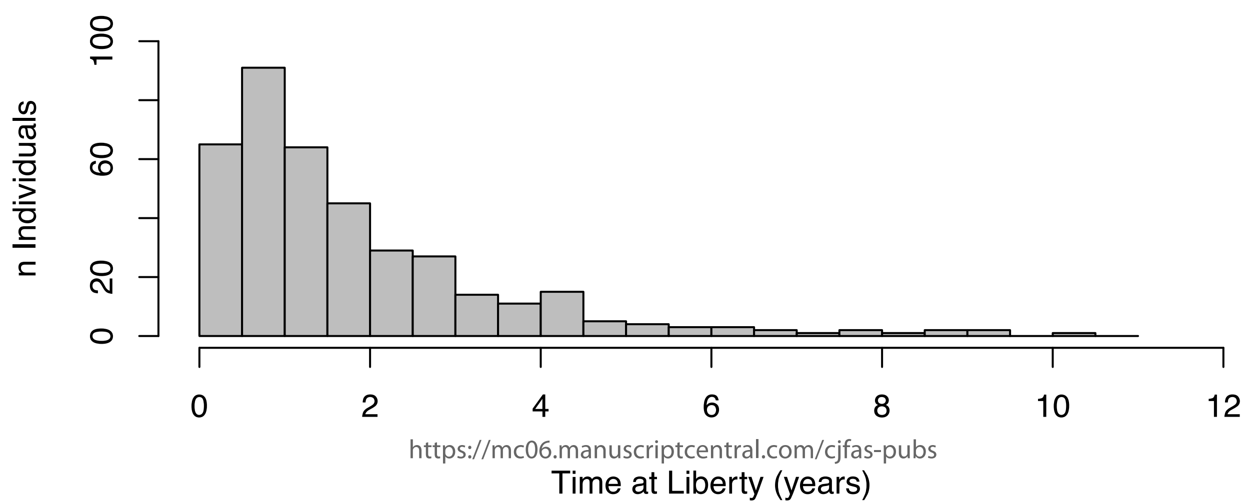

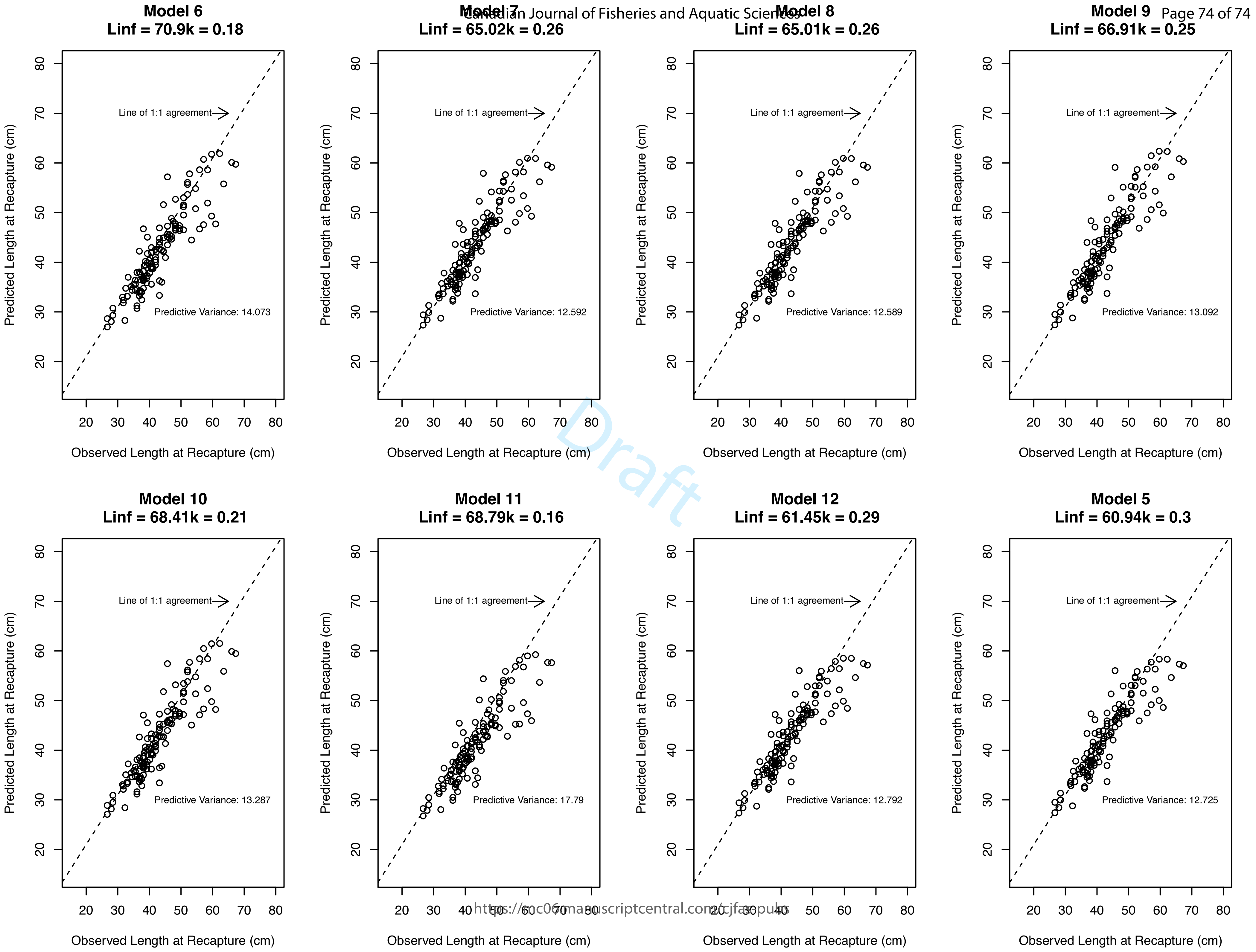

Model 6
Linf = 70.9k = 0.18
Predictive Variance: 14.073
Model 7
Linf = 65.02k = 0.26
Predictive Variance: 12.592
Model 8
Linf = 65.01k = 0.26
Predictive Variance: 12.589
Model 9
Linf = 66.91k = 0.25
Predictive Variance: 13.092
Model 10
Linf = 68.41k = 0.21
Predictive Variance: 13.287
Model 11
Linf = 68.79k = 0.16
Predictive Variance: 17.79
Model 12
Linf = 61.45k = 0.29
Predictive Variance: 12.792
Model 5
Linf = 60.94k = 0.3
Predictive Variance: 12.725
Line of 1:1 agreement
Predicted Length at Recapture (cm)
Observed Length at Recapture (cm)
20 30 40 50 60 70 80